Tunable $Ba_{0.5}Sr_{0.5}TiO_3$ film bulk acoustic resonators using SiO_2/Mo Bragg reflectors*

Yang Tian-Ying(杨天应)†, Jiang Shu-Wen(蒋书文)‡, Li Ru-Guan(李汝冠), and Jiang Bin(姜 斌)

State Key Laboratory of Electronic Thin Films and Integrated Devices, University of Electronic Science and Technology of China, Chengdu 610054, *China*

(Received 4 March 2012; revised manuscript received 28 April 2012)

Tunable and switchable $Ba_{0.5}Sr_{0.5}TiO_3$ film bulk acoustic resonators (FBARs) based on SiO_2/Mo Bragg reflectors are explored, which can withstand high temperature for the deposition of $Ba_xSr_{1-x}TiO_3$ (BST) films at 800 °C. The dc bias-dependent resonance may be attributed to the piezoelectricity of the BST film induced by an electrostrictive effect. The series resonant frequency is strongly dc bias-dependent and shifts downwards with dc bias increasing, while the parallel resonant frequency is only weakly dc bias-dependent and slightly shifts upwards at low dc bias (< 45 V) while downwards at higher dc bias. The calculated relative tunability of shifts at series resonance frequency is around -2.3% and the electromechanical coupling coefficient is up to approximately 8.09% at 60-V dc bias, which can be comparable to AlN FBARs. This suggests that a high-quality tunable BST FBAR device can be achieved through the use of molybdenum (Mo) as the high acoustic impedance layer in a Bragg reflector, which not only provides excellent acoustic isolation from the substrate, but also improves the crystallinity of BST films withstanding higher deposition temperature.

Keywords: $Ba_xSr_{1-x}TiO_3$, tunable film bulk acoustic wave resonator, ferroelectric, acoustic Bragg reflector

PACS: 68.60.Bs, 72.50.+b **DOI:** 10.1088/1674-1056/21/10/106801

1. Introduction

Thin film bulk acoustic resonators (FBARs) using piezoelectric aluminum nitride (AlN) and zinc oxide (ZnO) have been widely used in mobile phones for duplexer and filter in radio frequency (RF) front ends. These components have advantages of small size, low insertion loss, high power carrying capacity, and integration with complementary metal–oxide semiconductor (CMOS) technology.[1] However, with the development of wireless communication technology, it is essential to require a filter[2] which can be tuned to accommodate operation in different frequency bands for a mobile phone with multiple functions. Tunable FBARs using the traditional piezoelectric materials, AlN and ZnO, are not very promising due to a very low tuning or tuning speed, and power consumption issues.[3,4] Tunable FBARs of lead zirconate titanate (PZT) with relatively high tunability have been reported; but one problem for practical applications is the hysteresis due to the polar phase of the material.[5,6] Compared with the traditional materials, $Ba_xSr_{1-x}TiO_3$ (BST) film is in paraelectric phase at room temperature without piezoelectricity; however, under an applied dc bias, BST film induces piezoelectric effect due to electrostriction, which is nonlinear[7] with respect to the mechanical deformation. Tunable FBARs,[8,9] filters,[10,11] and RF switches[12,13] have been reported using BST film based on this feature, which makes integrated tunable circuit components possible for wireless communication systems with low loss, high quality factor, and low control voltage.

A solidly mounted thin-film bulk acoustic resonator (SMR)[14–18] has a high mechanical strength, where the Bragg reflector usually consists of many quarter wavelength layers of alternating high and low acoustic impedances, providing the necessary acoustic isolation from substrates. The SMR structure provides zero acoustic impedance for the top interface and an acoustic impedance of almost zero for the bottom interface where the acoustic reflector layer reflects the acoustic wave back to the piezoelectric layer. During resonator operation, at any of the interfaces between

*Project supported by the National Natural Science Foundation of China (Grant Nos. 60871049 and 50972024).

†Corresponding author. E-mail: yangtianying521@163.com

‡Corresponding author. E-mail: jiangsw@uestc.edu.cn

© 2012 Chinese Physical Society and IOP Publishing Ltd

high and low impedance layers, a large percentage of the waves will be reflected, which are superposed up with the correct wave. It presents an apparent zero impedance at the interface as the case in the ideal free air resonator structure. Compared with the deposition of AlN film, the deposition of the high-quality BST crystalline films requires a relatively high temperature, typically above 600 °C.[19] So it is essential to avoid oxidation or diffusion of Bragg reflectors withstanding the high temperature in oxygen atmosphere required for the deposition of high-quality BST films. At present, various kinds of SMRs fabricated on Ag/SiO_2,[20] W/SiO_2,[19,21] AlN/SiO_2,[22] and Pt/SiO_2[23] reflectors have been reported. However, most of these Bragg reflectors do not withstand the high deposition temperature required for BST. Aluminium (Al), platinum (Pt), tungsten (W), and gold (Au) metals each have a low acoustic impedance, which is disadvantageous for their use in Bragg reflectors. Compared with these Bragg reflector materials, molybdenum (Mo), having a high acoustic impedance, is suggested to be more suitable for high-quality SMRs. In this paper, the SiO_2/Mo Bragg reflectors are utilized where the BST films are deposited by magnetron sputtering at 800 °C, the resulting BST thin film bulk acoustic resonators show excellent tunable properties. The shift at series resonance frequency is observed to be −2.3% under an applied 60-V dc bias, and the maximum electromechanical coupling coefficient is approximately 8.09%, which is comparable to that of AlN FBARs.[24,25]

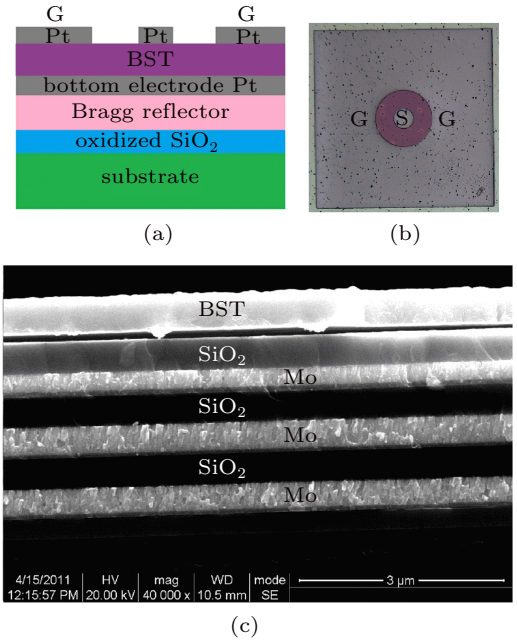


Fig. 1. (a) Schematic structure, (b) the top view, and (c) the cross-sectional SEM image of an FBAR device. The cross-sectional SEM image was achieved before the top electrode was deposited.

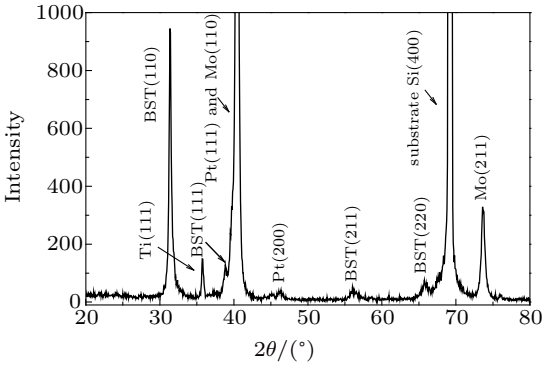


Fig. 2. XRD pattern of the deposited BST film for the FBAR.

2. Experiment

The devices were fabricated starting with a silicon wafer, therefore allowing future integration of other passive microwave components. The wafer surface was dry oxidized resulting in 300-nm thick SiO_2 layer. The FBARs were implemented as solidly mounted devices with a Bragg reflector, as shown in Fig. 1. The Bragg reflector was composed of three layers of alternating high and low acoustic impedances (Mo/SiO_2). The Mo and SiO_2 layers were deposited by electron beam evaporation onto the silicon substrate at 300 °C. Prior to the preparation of the film, an approximately 20-nm Ti adhesion layer was evaporated on each layer to improve the adhesion of the film. Square-shaped Pt bottom electrodes with a 260-μm long edge were patterned by evaporation and using the lift-off process. The BST films were deposited by radio frequency (RF) magnetron sputtering using a paraelectric $Ba_{0.5}Sr_{0.5}TiO_3$ target at 800 °C, followed by annealing at 800 °C for 2 h to further improve the crystallinity of the ferroelectric films. In our experiment, the structural phase composition and crystallization of the device were characterized by X-ray diffraction (XRD), using a Dandong DX-2000 type X-ray diffractometer with Cu Ka radiation. The X-ray wavelength is 0.15406 nm. The sharp and strong BST peaks in the XRD pattern shown in Fig. 2 reveal the excellent crystallinity of the prepared BST thin films. The Pt top electrode was designed with a circular radius of 28 μm. Effective capacitive coupling to the bottom electrode

is provided by the large area outer electrode, which is also suitable for measurement using cascade ground-signal-ground microprobes. The preparation procedure for the Pt top and outer electrodes was identical with that of the bottom electrodes. A top-view photograph of a fabricated FBAR device is shown in Fig. 1(b). The cross-sectional scanning electron microscope (SEM) image in Fig. 1(c) indicates that all layers in the reflector stack are still well defined after the high temperature BST film growth. Table 1 gives the thickness of each layer of the prepared BST FBARs upward from the silicon substrate. The thickness of the top electrode was tested by using a Dektak 150 surface profilometer.

Table 1. Layer thickness of the BST FBAR device upwards from the substrate.

Layer	Mo	SiO_2	Mo	SiO_2	Mo	SiO_2	Pt	$Ba_{0.5}Sr_{0.5}TiO_3$	Pt
Thickness/nm	39	4212	406	399	316	412	110	530	80
Error/nm	11	12	13	12	14	15	10	14	80

3. Results and discussion

Single port reflection coefficient measurements were fulfilled in a frequency range of 2.5 GHz–4.5 GHz using ground-signal-ground microprobes and an E5071C network analyzer. The return loss of a BST film bulk acoustic wave resonator with a Mo/SiO_2 Bragg reflector is shown in Fig. 3. At zero bias, there is no resonance. The reflection coefficient $S(1,1)$ is almost a constant of -1.6 dB, so the BST FBAR acts as a simple capacitor, which is possibly due to the BST film being in paraelectric phase without piezoelectricity. However, under an applied direct current (dc) voltage, the resonance is observed. This means that the BST FBAR is switched on or off depending on whether a dc bias is applied to the device or not. We also notice that the resonance becomes more pronounced and can be tuned by increasing the dc bias. The inset in Fig. 3 shows that the tunability of the resonator where the resonant frequency shifts upwards at low dc bias while downwards with dc bias increasing. When a 45-V dc bias is applied, the strongest resonance with a maximum frequency is detected and the return loss reduces to -30.7 dB. The field-dependent resonance may be attributed to the piezoelectricity of the BST film induced by the electrostrictive effect.

The bias-dependent tunabilty of the BST FBAR resonator can be further demonstrated in Fig. 4, which shows the magnitude of the measured input impedance of the resonator near the resonant frequency. The applied dc bias varies from 0 V to 60 V. The maximum in the input impedance magnitude corresponds to the parallel resonant frequency f_p, and the minimum input impedance corresponds to the series resonant frequency f_s. The input impedance magnitudes of parallel resonant frequency under different dc bias voltages quickly increase with dc bias increasing. The max input impedance magnitude of parallel resonant frequency under 60-V dc bias can be up to 65 Ω. The result can directly indicate that the electrostriction in BST FBAR increases with dc bias increasing.

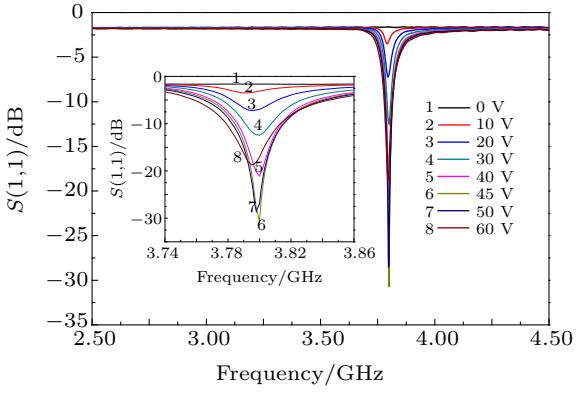


Fig. 3. (colour online) Measured return losses of the tunable bulk acoustic wave resonator at different dc bias voltages and the inset displays the magnification near the resonance frequency, showing the tunability of the device.

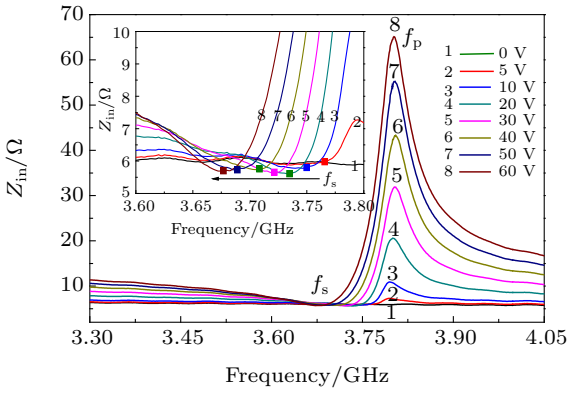


Fig. 4. (colour online) Magnitudes of the input impedance (Z_{in}) at different dc bias voltages with the inset displaying a magnification of the series resonant frequency, and so showing the tunability of the device.

While the minimum input impedance, corresponding to series resonant frequency f_s, changes a little.

The parallel and series resonant frequencies each as a function of applied dc bias are plotted in Fig. 5. The series resonant frequency f_s is strongly bias-dependent and decreases obviously, which is nearly linear from 3.760 GHz at 5 V to 3.673 GHz at 60 V dc bias, as can be seen from Fig. 5. The calculated relative tunability of the shift at series resonance frequency is around −2.3%. The tuning features of the series resonant frequency can be explained by combining the classical results of the FBAR theory of ferroelectrics. In the induced piezoelectricity, the electromechanical coupling coefficient k_t^2 and the elastic constant are dc bias dependent,[4] which leads to the tuning of the series resonance frequency. However, the parallel resonant frequency f_p shows much weaker dc bias dependency. The parallel resonance frequency f_p shifts upwards slightly with bias increasing from 3.795 GHz at 5-V dc to 3.805 GHz at 45-V dc, then tremendously decreases to lower frequencies. The shifts toward lower frequencies usually may be attributed to the increased thickness of ferroelectric film due to bias-induced electrostrictive effect. In this study, however, we note that the upshift of parallel resonant frequency at lower bias dc (< 45 V) is also observed. This positive tunability has been theoretically predicted based on Landau theory[26,27] and electromechanical equations,[3] which suggests a correlation with the negative nonlinear electrostriction coefficient dependent on the structural phase of the ferroelectric material.

The electromechanical coupling coefficient k_t^2 was extracted from

$$k_t^2 = \frac{\pi}{2}\frac{f_s}{f_p}\tan\left[\frac{\pi}{2}\left(\frac{f_p - f_s}{f_p}\right)\right],$$

where f_s and f_p are the series and parallel resonant frequencies, respectively, and plotted in Fig. 5 as well. The electromechanical coupling coefficient k_t^2 is nearly linear with respect to the increase of dc bias. The value at 60-V dc bias corresponds to 8.09% of a k_t^2 value, which is comparable to that of an AlN FBAR.[24,25] This suggests that the significant improvement on electromechanical coupling coefficient in a BST FBAR device can be achieved through using molybdenum (Mo) as high acoustic impedance layer in the Bragg reflector, which not only provides excellent acoustic isolation from the substrate, but also improves the crystallinity of BST films withstanding higher deposition temperature.

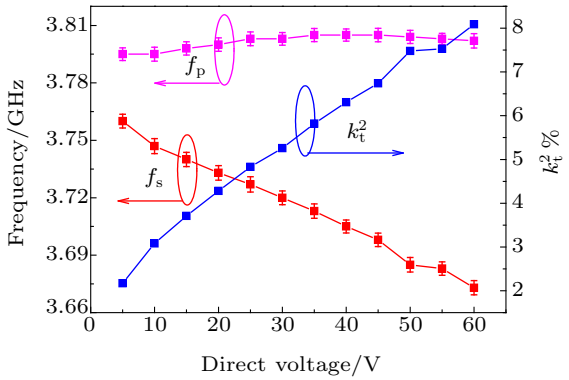


Fig. 5. (colour online) Electromechanical coupling coefficient k_t^2, series resonance frequency f_s, and parallel frequency f_p versus dc bias voltage. The dc bias increases from 5 V to 60 V in steps of 5 V.

Figure 6 shows the quality factor of the FBAR resonator, which is calculated from $Q = f/2(\partial\phi/\partial f)|_{\phi=f_{res}}$, where ϕ and f_{res} are the phase and the resonance frequency, respectively. Over the wide bias range the quality factor is above 70 with a maximum value of 82 at 45-V dc bias. The limited quality factor of our device can be improved by using an appropriately designed layout where the test probe tip is off the device to free the pressure applied by the tip, and using thinner top and bottom electrodes. A further study is still in progress.

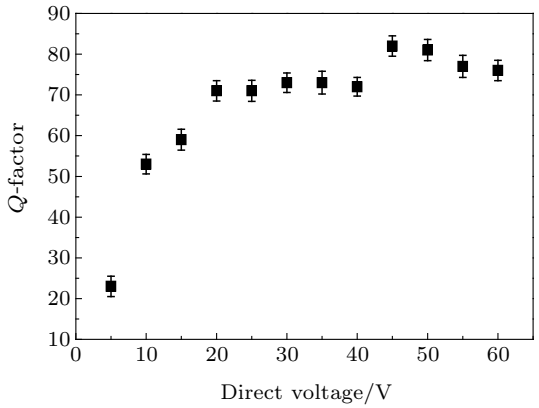


Fig. 6. Variation of quality factor of a tunable FBAR device with dc bias voltage.

Table 2 lists the properties of the solidly mounted BST FBARs with different Bragg reflectors. The measurement results of our device with a SiO_2/Mo reflector are given in the last row. Compared with the devices with other reflectors, our device demonstrates improved tunability and electromechanical coupling coefficient.

Table 2. Comparisons among the performances of the solidly mounted thin film bulk acoustic resonators with different Bragg reflectors. The tunabilities with superscript are derived from the results in the references, and — denotes the electromechanical coupling coefficient k_t^2 that is not given here.

$Ba_xSr_{1-x}TiO_3$	Bragg reflectors	Deposition temperature/°C	Resonant frequency/GHz	Tunability of f_s(%)	k_t^2/(%)	Quality factor
$x = 0.25$[19]	SiO_2/W	600	5.14	−1.5	—	150–200
$x = 0.25$[20]	SiO_2/Au	650	4	−1.2	0.5	120
$x = 0.25$[21]	SiO_2/W	600	5	$-0.9^{@}$	—	250
$x = 0.25$[22]	SiO_2/AlN	> 600	5	$< -1^{@}$	3	135
$x = 0.5$	SiO_2/Mo	800	3.8	−2.3	8.09	82

4. Conclusion

Using molybdenum (Mo) as high acoustic impedance layer for BST solidly mounted thin film bulk acoustic resonators not only provides excellent acoustic isolation from the substrate, but also improves the crystallinity of BST films due to high deposition temperature (800 °C). The cross-sectional SEM image of the device indicates that the layers in the reflector stack are still well defined after BST film growth. The reflection coefficients $S(1,1)$ can be reduced to −30.7 dB under 45-V dc bias, which reveals the strong electrostriction effect of BST ferroelectric film. The series resonant frequency is strongly dc bias-dependent and shifts downwards with the increase of dc bias, while the parallel resonant frequency is only weakly dc bias-dependent and shifts upwards with the increase of dc bias at low dc bias (< 45 V). The tunability is consistent with that from previous theory. Above 45 V, the parallel resonant frequency decreasing tremendously to lower frequencies usually may be attributed to the increased thickness of ferroelectric film due to the bias-induced electrostrictive effect. The calculated relative tunability of shifts at series resonance frequency is around −2.3% and the electromechanical coupling coefficient is up to approximately 8.09% at 60-V dc bias. The bias-dependent quality factor is far lower than that of single crystal BST. Thus there is room for substantial improvement of the quality factor of the resonator to meet the need of tunable filters.

References

[1] Qin J R, Chen S M, Liang B and Liu B W 2012 *Chin. Phys.* B **21** 029401

[2] Zhang C X, Nie Y H and Liang J Q 2008 *Chin. Phys.* B **17** 2670

[3] Berge J, Norling M, Vorobiev A and Gevorgian S 2008 *J. Appl. Phys.* **103** 064508

[4] Vendik I B, Turalchuk P A, Vendik O G and Berge J 2008 *J. Appl. Phys.* **103** 014107

[5] Schreiter M, Gabl R, Pitzer D, Priming R and Wersing W 2004 *J. Eur. Ceram.* **24** 1589

[6] Noeth A, Yamada T, Sherman V O, Muralt P, Tagantsev A K and Setter N 2007 *IEEE Trans. Ultrason. Ferroelectr. Freq. Control* **54** 2487

[7] Guo Z R, Yang Z Q, Yin B X and Sun M Z 2010 *Chin. Phys.* B **19** 116201

[8] Noeth A, Yamada T, Muralt P, Tagantsev A K and Setter N 2010 *IEEE Trans. Ultrason. Ferroelectr. Freq. Control* **57** 378

[9] Tappe S, Böttger U and Waser R 2004 *Appl. Phys. Lett.* **85** 624

[10] Turalchuk P, Vendik I, Vendik and Berge J 2008 *Proceedings of the 38th European Microwave Conference,* October 27–31, 2008, Amsterdam, Netherlande, p. 1695

[11] Zhu X E, Lee V, Phillips J and Mortazawi A 2009 *IEEE Microw. Wireless Componen. Lett.* **19** 359

[12] Zhu X E, Phillips J D and Mortazawi A 2007 *Proceedings of International Microwave Symposium,* June 3–8, 2007, Hawaii, USA, p. 671

[13] Mikhailov A, Prudan A, Ptashnik S, Samoilova T and Kozyrev A 2010 *Proceedings of the 40th European Microwave Conference,* September 28–30, 2010, Paris, France, p. 791

[14] Zhao H J 2012 *Chin. Phys.* B **21** 087104

[15] Xiong K, Xiao X, Hu Y T, Li Z Y, Chu T, Yu Y D and Yu J Zh 2012 *Chin. Phys.* B **21** 074203

[16] Yang Y M, Wang J F, Xia S, Bai P, Li Z, Wang J, Xu Z and Qu S B 2011 *Chin. Phys.* B **20** 014101

[17] Huang Q Z, Yu J Z, Chen S W, Xu X J, Han W H and Fang Z C 2008 *Chin. Phys.* B **17** 2562

[18] Meng X Z, Wang M Z and Ren Z M 2011 *Chin. Phys.* B **20** 050702

[19] Vorobievl A and Gevorgian S 2010 *IEEE Microwave Symp. Digest, MTTS Int.* **57** 379

[20] Berge J, Vorobiev A, Steichen W and Gevorgian S 2007 *IEEE Trans. Microw. Wireless Comput. Lett.* **17** 655

[21] Vorobieva A and Gevorgian S 2010 *Appl. Phys. Lett.* **96** 212904

[22] Vorobiev A, Berge J, Norling M and Gevorgian S 2010 *Proceedings of the 10th Topical Meeting on Silicon Monolithic Integrated Circuits in RF Systems,* January 11–13, New Orleans, USA, p. 41

[23] Saddik G N, Boesch D S, Stemmer S and York R A 2007 *Appl. Phys. Lett.* **91** 043501

[24] Volatier A, Defaÿ E, Aïd M, N'hari A, Ancey P and Dubus B 2008 *Appl. Phys. Lett.* **92** 032906

[25] Sanchez S, Rhun G L, Suhm A and Defaÿ E 2010 *Proceedings of the 40th European Microwave Conference,* Septembe 28–30, Paris, France, p. 799

[26] Noeth A, Yamada T, Sherman V O, Muralt P, Tagantsev A K and Setter N 2007 *J. Appl. Phys.* **102** 114110

[27] Noeth A, Yamada T, Tagantsev A K and Setter N 2008 *J. Appl. Phys.* **104** 094102